Geochemistry Geophysics Geosystems G3
AN ELECTRONIC JOURNAL OF THE EARTH SCIENCES
Published by AGU and the Geochemical Society

Characterization
Volume 8, Number 7
25 July 2007
Q07008, doi:10.1029/2006GC001406
ISSN: 1525-2027

Toward forward modeling for paleoclimatic proxy signal calibration: A case study with oxygen isotopic composition of tropical woods

M. N. Evans
Laboratory of Tree-Ring Research, University of Arizona, 105 West Stadium, Tucson, AZ 85721, USA (mevans@ltrr.arizona.edu)

[1] A forward model of the oxygen isotopic composition ($\delta^{18}O$) of wood cellulose is parameterized for time series prediction in tropical environments and driven with meteorological data observed at La Selva Biological Research Station, Costa Rica, for 1985–2001. Monthly-resolution model results correlate modestly ($r = 0.34$, $p < 0.05$) with observed isotopic data, with higher correlation ($r = 0.45$, $p < 0.01$) over the earliest 10 years of comparison and nonsignificant correlation over the most recent 6 years of record. Analysis of model output for La Selva suggests that isotopic variations are strongly controlled by rainfall amount. The model simulates an analogous but stronger than observed negative isotopic anomaly associated with positive July–September rainfall anomalies during El Niño–Southern Oscillation (ENSO) warm phase event years. Simulated tree isotope data for the global tropics suggest that a network of well-replicated data series from selected locations may resolve the large-scale precipitation anomaly pattern associated with ENSO.

Components: 7115 words, 4 figures, 3 tables.

Keywords: dendroclimatology; stable isotopes; forward model; precipitation; Monte Carlo; tropics.

Index Terms: 0466 Biogeosciences: Modeling; 0454 Biogeosciences: Isotopic composition and chemistry (1041, 4870); 0473 Biogeosciences: Paleoclimatology and paleoceanography (3344, 4900).

Received 30 June 2006; **Revised** 6 February 2007; **Accepted** 27 February 2007; **Published** 25 July 2007.

Evans, M. N. (2007), Toward forward modeling for paleoclimatic proxy signal calibration: A case study with oxygen isotopic composition of tropical woods, *Geochem. Geophys. Geosyst.*, *8*, Q07008, doi:10.1029/2006GC001406.

1. Introduction

[2] The natural variability and response of the tropical hydrological cycle to anthropogenic forcing is a key uncertainty in climate change prediction studies [*Subcommittee on Global Change Research*, 2003]. In support of projects exploiting tree rings as archives of hydrologic variations, J. S. Roden and colleagues modeled the environmental controls on the oxygen isotopic composition of the α-cellulose component of wood [*Roden et al.*, 2000]. Their model was recently modified and summarized by *Barbour et al.* [2004] (hereafter referred to as *BRFE04*) as

$$\Delta_c = \Delta_l(1 - p_x p_{ex}) + \epsilon_c$$

Here Δ refers to oxygen isotopic composition measured relative to the oxygen isotopic composition of "source water" taken up by the plant,

$$\Delta_c = 1000\left(\frac{R_{cellulose}}{R_s} - 1\right)$$

with $R \equiv \frac{^{18}O}{^{16}O}$, subscript indicating the relevant material, and is expressed in per mil (‰) units. The isotopic composition of the source water, $\delta^{18}O_s$, which itself can vary with meteorological and environmental conditions, is referenced to the isotopic composition of Standard Mean Ocean Water (SMOW); hence the cellulose isotopic composition relative to SMOW is

$$\delta_c = 1000\left(\frac{(\frac{\Delta_c}{1000}+1)R_s}{R_{SMOW}}\right).$$

[3] In essence, the isotopic composition of cellulose is determined by the oxygen isotopic composition of soil water, leaf evaporative processes, and the equilibrium fractionation incurred during cellulose biosynthesis ϵ_c. A fraction $(1-p_x p_{ex})$ of the source water is isotopically modified by evaporative processes at the leaf. The factor $p_x p_{ex}$ reflects re-equilibration of the exchangeable cellulose oxygen fraction p_{ex} with stem water, and the fraction p_x of unenriched stem water at the site of cellulose biosynthesis [*BRFE04*]. The equilibrium fractionation incurred during cellulose biosynthesis, due to fractionation between carbonyl and water oxygen, is ϵ_c. Δ_l is calculated from the isotopic composition of water at the evaporation site, Δ_e, and the Peclet effect:

$$\Delta_l = \left\{(1+\epsilon^*)\left[1+\epsilon_k+(\Delta_{wva}-\epsilon_k)\frac{e_s}{e_i}\right]-1\right\}\left(\frac{1-e^{-\wp}}{\wp}\right)$$

Here, ϵ_k and ϵ^* are temperature-dependent kinetic and equilibrium liquid-vapor fractionation factors, Δ_{wva} is the isotopic composition of atmospheric water vapor, and e_s and e_i are the leaf surface and leaf interstitial water vapor pressures, respectively. The dimensionless Peclet number $\wp = \frac{LE}{CD}$ is calculated from effective evaporative pathway length L, evaporation rate E, molar density of water C, and diffusivity of $H_2^{18}O$ in water. The formulation for Δ_l reflects dependence of leaf-level evaporation on leaf temperature, isotopic composition of water vapor, leaf-air humidity gradient, and both equilibrium and disequilibrium isotope effects of transpiration. Using this model (made freely available by *BRFE04* for download from ftp://ecophys.biology.utah.edu/tree_ring/), known values of relative humidity, air temperature, leaf temperature, source water and atmospheric water vapor $\delta^{18}O$, and 9 biophysical variables and parameters [*Barbour et al.*, 2004], Δ_l and Δ_c can be predicted.

[4] We recently described [*Evans and Schrag*, 2004] (hereafter *ES04*) an application of this system to development of chronological and paleoclimatological estimates from tropical trees lacking visible ring structure. A heuristic description of the argument is given by *ES04*, but the fundamental idea is this: the annual cycle of precipitation amount should be recorded in intra-annual measurements of the $\delta^{18}O$ measured on the α-cellulose component of tropical woods [*Verheyden et al.*, 2004; *Poussart et al.*, 2004]. Potentially, replicated multicentury proxy data series of precipitation variations could be developed for regions of the terrestrial tropics largely unobserved prior to the mid-20th century. But can the model of *Barbour et al.* [2004] be used to explicitly test whether actual isotopic measurements from tropical trees are consistent with this interpretation? I address this question using a direct intercomparison of simulated and observed oxygen isotope time series from a well-observed site in Central America. The environment is quite different from that in which the *BRFE04* model was developed and tested, and prior work at the site enables specification of many model parameters based on previously published data. The data-model intercomparison therefore represents a rigorous test of the model. I will also suggest more generally that the forward modeling of proxy observations is an important approach for linking the interpretation of paleoenvironmental proxy data to the physical, chemical and biological first principles underlying the proxy system.

2. Materials and Methods

2.1. Proxy Observations

[5] As the modeling target I chose an age-modeled $\delta^{18}O$ data series developed by *ES04* from a 16-year-old plantation Hyeronima alcorneides sampled in March 2001 at the La Selva Biological Research Station of the Organization for Tropical Studies, Puerto Viejo de Sarapiqui, Costa Rica (10.4°N, 84°W, 40 m) [*Butterfield and Espinosa*, 1997]. Sample preparation, analysis, and isotopic data are described by *ES04*; subsequent experiments indicate no significant difference in $\delta^{18}O$ values obtained from the analytical chemistry used in this work and more classical techniques for cellulose extraction (K. J. Anchukaitis et al., Rapid cellulose processing for high-resolution isotope dendroclimatology, manuscript in preparation, 2007). Measurement precision is 0.3, estimated from repeated measurements of a working standard material. The data series was age modeled [*ES04*]

by assigning isotopic minima to July of each year, corresponding to climatologically maximum precipitation at La Selva's meteorological stations [*Brenes*, 2003] over the 1985–2001 period, and working backward in time from the most recent growth to the innermost material from the sample core. Intra-annual sample ages were estimated for each data point via continuous, piecewise linear interpolation to monthly resolution; no seasonal or annual growth hiatus was assigned. *ES04* estimated age model error in the resulting data series to be ±2 years.

2.2. Model Parameterization

[6] We seek a first-principles model of the link between environmental conditions and the oxygen isotopic composition of cellulose, $\delta^{18}O_c$, which can be driven by a small set of readily available meteorological data. In the tropics, several *BRFE04* inputs and variables may be parameterized as functions of temperature, precipitation, and relative humidity in the following manner.

[7] 1. Following *Linacre* [1964], and in the absence of a species-specific equation, we estimate leaf temperature as a linear function of air temperature:

$$T_{leaf} = c_1 + c_2 T_{air}$$

where c_1 and c_2 are empirically determined constants. Note that this equation closely simulates Linacre's meta-analysis of 42 published studies on a range of species and environments. It is intended to parameterize the balance between leaf sensible heating and evaporative cooling, which can result in leaf temperature either higher than or lower than air temperature.

[8] 2. Following *Bowen and Wilkinson* [2002, and references therein] for the relationship between amount and isotopic composition of rainfall, we estimate $\delta^{18}O_s$ as

$$\delta^{18}O_s = c_3 + c_4 P$$

where c_3 and c_4 are empirically determined constants, and P is precipitation. The parameterization mimics the observed tendency of tropical rainfall to behave approximately as a Rayleigh distillation process, in which increasing amounts of convective rainfall are increasingly isotopically depleted of the heavy isotope-labeled $H_2^{18}O$ molecule [*Fairbanks et al.*, 1997]. It should be noted that the slope and regression of the amount effect relationship employed in this case study pertain to monthly resolution simulations. Using the model with different resolution input data and for different tropical locales may require different choices for c_3 and c_4. However, it is encouraging that *Lachniet and Patterson* [2006] found that the amount effect observed in Panamanian precipitation was similar for monthly and annual timescales.

[9] 3. The calculation of Δ_l requires an estimate of the oxygen isotopic composition of water vapor, $\delta^{18}O_{wva}$. We estimate the temperature of condensing precipitation T_c as

$$T_c = -c_5 c_6 + 273.15$$

where T_c is in Kelvins, c_5 is the condensation level (Km) and c_6 is the moist adiabatic lapse rate (c_6 = 6K/Km [*Wallace and Hobbs*, 1977]). The condensation level c_5 is chosen to place equilibration of vapor and precipitation above the boundary layer but not as high as the tropical tropopause (about 200 mb [*Peixoto and Oort*, 1996]), to allow for unmodeled effects of droplet re-evaporation on the isotopic composition of precipitation and water vapor. The temperature-dependent liquid-vapor fractionation factor is calculated as (*Majoube* [1971] referenced by *Gonfiantini et al.* [2001]):

$$\alpha_{LV} = \frac{1137}{T_c^2} - \frac{0.4156}{T_c} - 0.00207$$

and isotopic composition of atmospheric water vapor is

$$\delta^{18}O_{wva} = 1000\left(\frac{1}{\alpha_{LV}} - 1\right) + \delta^{18}O_s.$$

In practice the results are not sensitive to this parameterized estimation of $\delta^{18}O_{wva}$; the tropical Rayleigh model result of $\delta^{18}O_{wva} = \delta^{18}O_s - 8$ based on observed isotopes in tropical precipitation [*Fairbanks et al.*, 1997] gives quite similar results.

[10] 4. Following *Lohammar et al.* [1980] and *Aphalo and Jarvis* [1991], leaf stomatal conductance (G_s) varies inversely with leaf–air saturation vapor pressure deficit (D_s). Here, leaf saturation vapor pressure $e_{leaf,sat}$ is estimated from leaf temperature [*Bolton*, 1980], and vapor pressure of ambient air e_{air} is estimated from saturation vapor pressure of air at observed T_{air} and observed relative humidity. D_s is then estimated as

$$D_s = e_{leaf,sat} - e_{air}$$

and stomatal conductance G_s is estimated using the relationship

$$G_s = \frac{c_7}{D_s} + c_8$$

Monthly averages of measured stomatal conductance and vapor pressure deficit data for Hyeronima growing at La Selva [*Bigelow*, 2001; *Bigelow and Ewel*, 2006] were used to estimate parameters c_7 and c_8 (Table 2). We found that a linear relationship between G_s and D_s [*Aphalo and Jarvis*, 1991] produces very similar results over the calibrated and observed ranges for G_s and D_s; here we use the inverse relationship suggested by *Lohammar et al.* [1980] which is perhaps more realistic, and gives a slightly better fit ($r^2 = 0.73$, $N = 7$, $F = 13.6$, $p < 0.01$) to the observations with the same number of regression parameters.

[11] Transpiration is calculated [*Jarvis and McNaughton*, 1986] as

$$E = G_s D_s / P_{atm}$$

where P_{atm} is monthly mean atmospheric pressure, assumed to be constant at 1013 mb. Although monthly average surface atmospheric pressure could easily be added to the model as an input variable, its specification as a constant in tropical environments and on monthly timescales introduces negligible errors.

[12] 5. A two-component mixing model is assumed to represent the simulated environmental variations in the isotopic composition of tree α-cellulose, superimposed on a background state dictated by mean plant physiological and environmental characteristics. In this model, the time-average simulated $\delta^{18}O_c$ is set to equal the time-averaged observed $\delta^{18}O_c$,

$$\delta^{18}O_{c,model} = (1 - c_{10})c_9 + c_{10} \times \left[\delta^{18}O_{c,BRFE} - \left(\langle \delta^{18}O_{c,BRFE} \rangle - c_9\right)\right]$$

where $\langle \ldots \rangle$ indicates the time average, and the subscripts *model* and *BRFE* refer to 2-component-mixing modeled cellulose and *BRFE04*-simulated cellulose $\delta^{18}O$, respectively. Here the constant c_9 is interpreted as the observed mean of $\delta^{18}O_c$ at the study site, and c_{10} is the fraction of the root-mean-squared (RMS) variance which can be ascribed to environmental forcing as represented by precipitation, temperature and relative humidity variations. The mixing model allows correction for environments and/or species for which the tree is dependent upon both episodic precipitation and reliable soil or ground water, which together can result in a different observed and simulated mean cellulose $\delta^{18}O$. For example, as c_{10} approaches zero, the tree gets little moisture instantaneously from precipitation, the variance of $\delta^{18}O_{c,model}$ approaches zero, and the mean approaches the observed mean c_9, presumably reflecting the long term soil moisture–evaporation balance. As c_{10} approaches one, the tree gets all of its moisture from instantaneous precipitation, and the variance of $\delta^{18}O_{c,model}$ about the mean c_9 approaches that of $\delta^{18}O_{c,BRFE}$.

[13] 6. In the paleoclimatic context, many of the *BRFE04* variables and additional parameters will be unmeasured. For this reason, all chosen variables and tunable parameters of *BRFE04* were treated as time-independent constants (Tables 1 and 2). A Monte Carlo approach to estimation of uncertainty due to imperfect knowledge of all parameters was implemented. The model was run 1000 times, with each simulation made using all 17 parameters simultaneously and randomly perturbed with uniform probability density function from set values by up to a fixed percentage, c_{11}. The resulting estimates of the calculated variables were sorted, and ±2 standard deviation values for output model variables are reported. No attempt was made to optimize parameters on the basis of the Monte Carlo perturbation procedure. Instead, this approach merely efficiently samples the range in the 17-dimensional parameter space for assessment of sensitivity to the default parameter value choices.

[14] 7. For comparison with observations, which typically are made at about monthly time resolution and have an observational error of about 0.3 in $\delta^{18}O$ *ES04*, random Gaussian observational errors with standard deviation 0.3 have been added to all model results.

[15] The *BRFE04* model thus parameterized approaches the formulations of *Saurer et al.* [1997], *Anderson et al.* [2002], and *Waterhouse et al.* [2002], but allows variation due to additional biologically mediated processes [*Verheyden et al.*, 2004]. It can be run with input precipitation, temperature and relative humidity monthly resolution time series as independent variables. Model parameters held constant over time, input variables, and outputs are summarized in Tables 1–3. A MATLAB compatible function, allowing for manipulation of both input variables, parameters, and parameters treated as constants, is available from http://ic.ltrr.arizona.edu/Contrib.html or from the author upon request.

Table 1. *BRFE04* Variables and Default Values[a]

Variable	Description	Value
ϵ_s	diffusive fractionation through stomata (‰)	32
ϵ_b	diffusive fractionation through boundary layer (‰)	21
ϵ_c	equilibrium fractionation between carbonyl oxygen and water (‰)	27
g_{bl}	leaf boundary layer conductance (mmol/m^{2}s)	2100
L	effective length for the Peclet effect (m)	0.018
p_{ex}	mean proportion of exchangeable oxygen in cellulose (unitless)	0.42
p_x	proportion of xylem water in meristem (unitless)	1

[a] Variables described in detail by *Barbour et al.* [2004]. Note $\wp$ (section 1) is determined by E and L.

2.3. Meteorological Data

[16] Meteorological data have been recorded at La Selva Biological Research Station since the late 1950s, and daily data are available from an automated weather station for maximum temperature, minimum temperature, and precipitation since 1982. Relative humidity, maximum temperature, minimum temperature and precipitation have been monitored hourly and semi-hourly since 1992. All of these data were downloaded via anonymous ftp from OTS/OET and are gratefully acknowledged here [*Brenes*, 2003]. The semi-hourly data was filtered to remove outlier temperatures greater than 40°C, relative humidities above 100%, and data points for which all three variables were not measured simultaneously. Hourly temperature observations for 1982–2005 are used to relate daily minimum and maximum temperatures to mean daily temperatures:

$$T_{daily} = -3.56 \pm 0.32 + 1.13 \pm 0.012\langle T_{hourly}\rangle$$

with $\langle \ldots \rangle$ indicating the time average of hourly data from midnight to midnight. Note this regression is different in slope and intercept than obtained by taking the average of daily minimum and maximum values. Squared correlation of the variables is $r^2 = 0.90$ ($p < 0.0001$ with 11 effective degrees of freedom) and RMS error = 0.64°C. The regression has been used to estimate daily average temperature from the daily minimum and maximum temperature data for 1982–2001.

[17] For our purposes, daily temperature and precipitation data have been averaged to monthly resolution, first removing $>\pm 4\sigma$ outliers from the daily data. A multiple linear regression of relative humidity on temperature and precipitation for monthly averages over the 1992–2005 period gives the relation

$$RH(\%) = 102.98(\pm 8.50) + 0.012(\pm 0.0037)P(\text{mm}) - 0.69 \times (\pm 0.30)T(^\circ C)$$

which was used to reconstruct RH for the 1982–1992 and 1994–1995 periods of missing RH data,

Table 2. Model Variables, Parameters, and Default Values for *BRFE04* Time Series Extension[a]

Variable	Description	Value
T_{air}	monthly average air temperature (°C)	input variable
P	monthly average precipitation (mm)	input variable
RH	monthly average relative humidity (%)	input variable
c_1	y-intercept of $\delta^{18}O_s$ versus monthly average precipitation amount relationship (‰)	0.74
c_2	slope of $\delta^{18}O_s$ versus monthly average precipitation amount relationship (‰/mm)	−0.0285
c_3	y-intercept of leaf temperature versus air temperature relationship (°C)	10
c_4	slope of leaf temperature versus air temperature relationship (dimensionless)	23/33
c_5	height at which precipitation reaching ground is condensing (Km)	3
c_6	moist adiabatic lapse rate (K/Km)	6
c_7	first constant in regression of G_s on D_s (mb·mmol/m^2/s)	4290
c_8	second constant in regression of G_s on D_s (mmol/m^2/s)	−43
c_9	mean observed $\delta^{18}O_c$ for baseline correction (‰)	27.17
c_{10}	fraction RMS variance due to environmental forcing (dimensionless)	0.45
c_{11}	percent uncertainty in model parameters for Monte Carlo error estimation (%)	20

[a] Parameters c_1 and c_2 from *Lachniet and Patterson* [2006]; c_3 and c_4 from *Linacre* [1964]; c_5 and c_6 as described in text; c_7 and c_8 from *Bigelow* [2001] and *Bigelow and Ewel* [2006]. Parameters c_9 and c_{10} chosen by analysis of La Selva isotopic observations from *ES04*.

Table 3. Model Outputs

Output	Description
$\delta^{18}O_e$	$\delta^{18}O$ of water at evaporation sites (‰)
$\delta^{18}O_l$	$\delta^{18}O$ of leaf water (‰)
$\delta^{18}O_s$	$\delta^{18}O$ of sucrose (‰)
$\delta^{18}O_{c,BRFE}$	$\delta^{18}O$ of cellulose (‰)
$\delta^{18}O_{c,model}$	$\delta^{18}O$ of cellulose with soil water correction (‰)
mcerr	Monte Carlo estimated 5th and 95th percentile levels due to parameter uncertainty (‰)

on the basis of observed monthly averaged temperature and precipitation. Squared correlation of the variables is $r^2 = 0.47$ ($p < 0.05$ with 11 effective degrees of freedom) and RMS error = 2.5%. The reconstructed RH estimates have been adjusted to have the same mean and variance as the direct RH measurements, and the full time series is adjusted (−4.5%) to have the same mean as the La Selva grid point in the *New et al.* [2000]–based relative humidity product (Figure 4). Split period calibration and verification exercises for estimates of RH (results not shown) indicate the regression coefficients are stable to within error taking either 1992–2000 or 2000–2005 as calibration interval. However, squared verification correlations for these two calibration/verification exercises were $r^2 = 0.27$ and $r^2 = 0.61$, respectively, indicating a moderate degree of uncertainty in the RH estimates. The 1985–2001 monthly values for precipitation, temperature and relative humidity inputs to the model are shown in Figure 1. Note that the more poorly defined annual cycles in precipitation for 1995–2001 are apparently a replicated phe-

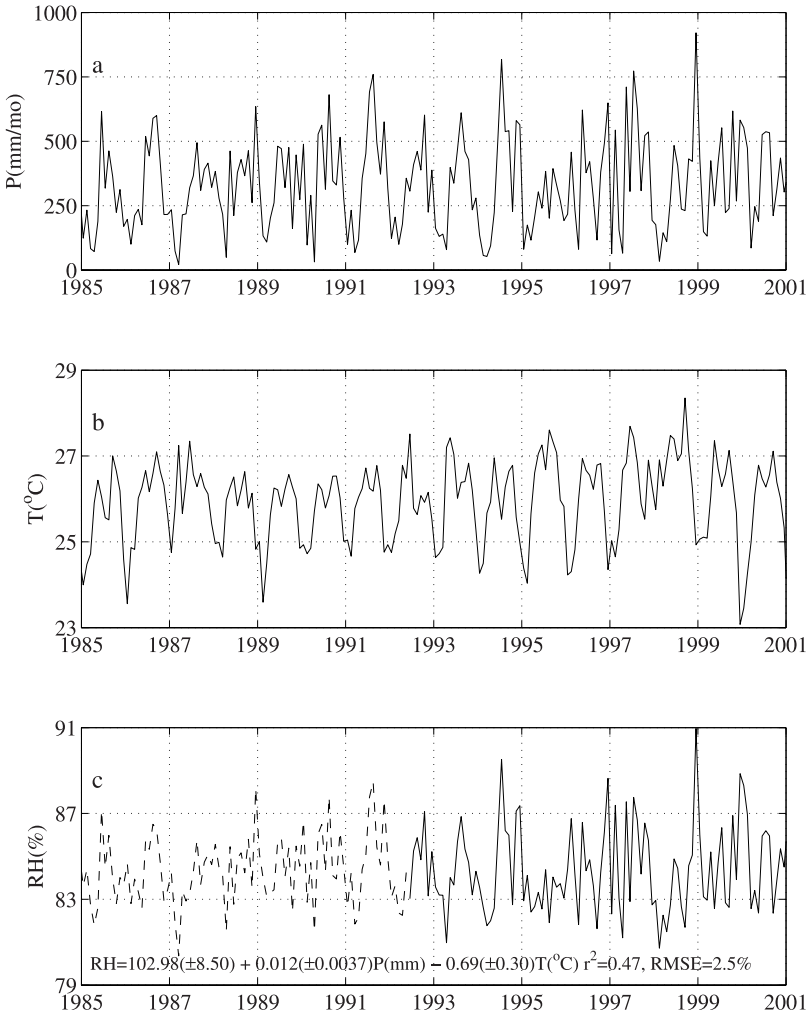

Figure 1. Monthly estimates of meteorological variables at La Selva Biological Research Station. (a) Monthly mean precipitation. (b) Monthly mean temperature. (c) Monthly mean relative humidity, based on multiple linear regression of relative humidity on temperature and precipitation for 1992–2005 period (estimated portion shown as dashed line; see text for details).

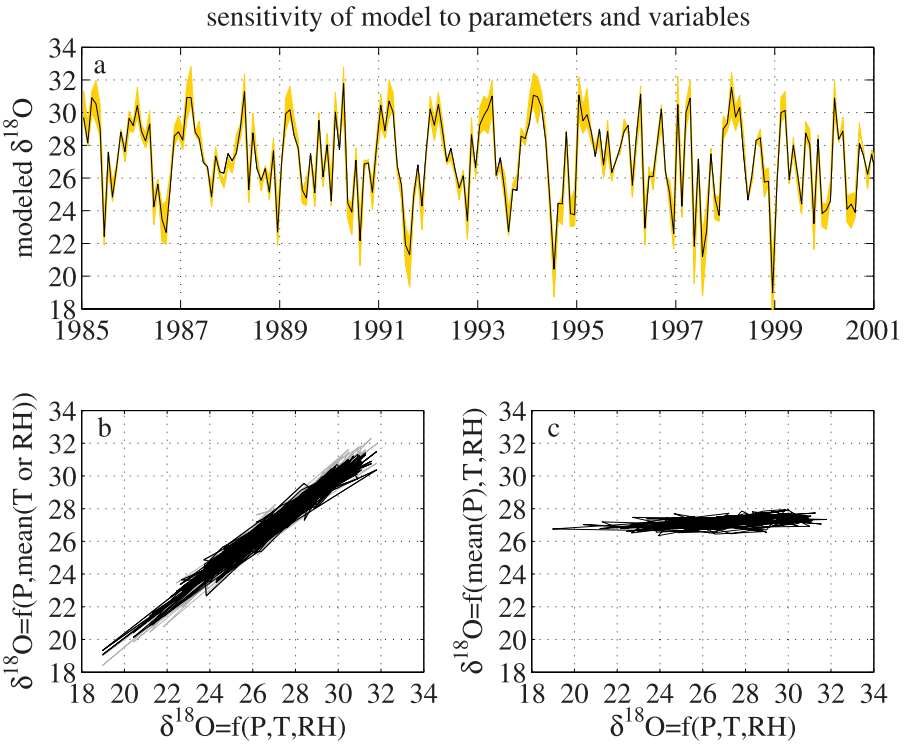

Figure 2. (a) Simulation of La Selva cellulose $\delta^{18}O_c$ (black line), and 5%–95% range in model results from Monte Carlo simulation of sensitivity to ±20% uncertainty in parameter choices (yellow area). The mean errors estimated due to parameter uncertainty (height of yellow coloration on plot) is 1.2. (b) Scatterplot of model results with temperature or relative humidity held constant at its mean 1985–2001 value versus full model simulation. Gray lines indicate results from relative humidity and temperature data with variances artificially inflated to 4 times observed or estimated variances. (c) Plot of model results with precipitation held constant at mean 1985–2001 value versus full model simulation.

nomenon; they are reproduced in meteorological data located 1Km from La Selva Station [*Bigelow*, 2001; *Bigelow and Ewel*, 2006] and in the 0.5° × 0.5° gridded precipitation data set of *New et al.* [2000]. The annual cycle of precipitation in 2.5° × 2.5° gridded data [*Xie and Arkin*, 1997] is more regular and suggests that the high intermonthly variations observed at La Selva for this period are probably a localized phenomenon.

3. Results

[18] The La Selva simulation of $\delta^{18}O_c$ is plotted in Figure 2a (black line). The difference between observed and simulated mean cellulose δ^{18}O values, prior to two-component mixing model calculations, was +5.1‰. The best fit of simulated to observed variance was with 45% (c_{10} = 0.45) of source water from precipitation; simulated and observed means and variances are stable to within about ±10% between the first and second halves of the data series. The Monte Carlo–estimated 2σ uncertainty range (vertical yellow bars), derived from 1000 model runs with simultaneous, random $\leq$±20% perturbations with uniform probability to all 17 model parameters, is about 1.2‰. The ±2σ range in values of $\delta^{18}O_{c,model}$ is 10.2‰

[19] Modeled ranges of leaf-air vapor pressure deficit (7.8–11 mb), stomatal conductance (350–510 mmol·m^{-2}·s^{1}) and evapotranspiration (3.7–3.9 mmol·m^{-2}·s^{1}) are in general agreement with ranges in published observations and model results [*Bigelow*, 2001; *Reich et al.*, 2004; *Bigelow and Ewel*, 2006; *Barbour et al.*, 2004]. Relative to model results produced holding these variables constant, variance introduced by these components of the model was less than 1% or 0.02‰. Variance of the term $p_{ex}p_x$ from 0.3–0.7 resulted in a damping of $\delta^{18}O_{c,model}$ by about 0.05 in amplitude (results not shown). A similar experiment inflating relative humidity variance by a factor of four also resulted in a negligible effect on the resulting $\delta^{18}O_{c,model}$ (Figure 2b).

[20] In Figure 2b, temperature and relative humidity are individually held constant at their 1985–2001

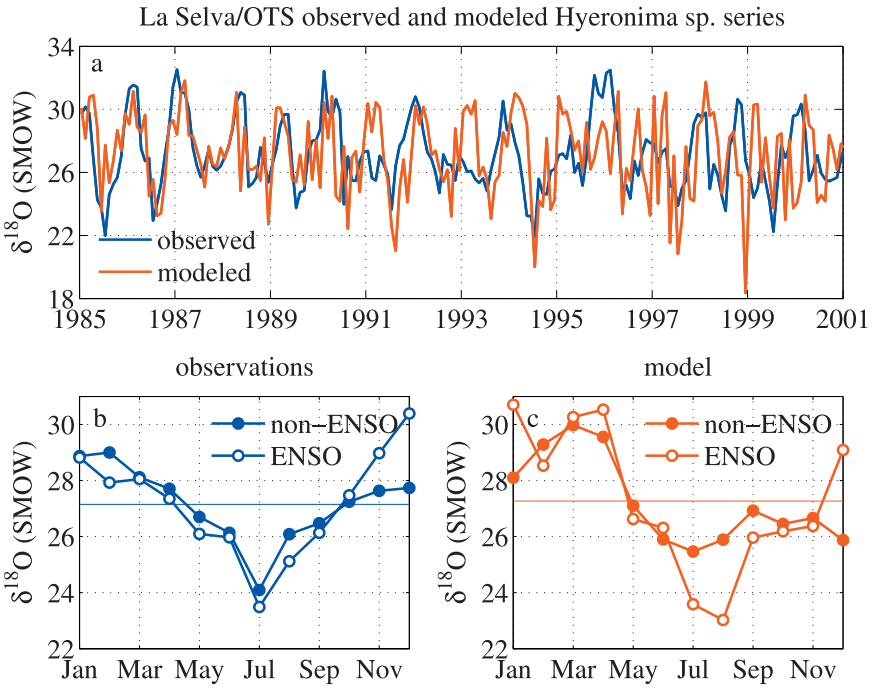

Figure 3. (a) Simulation of La Selva cellulose $\delta^{18}O_{c,model}$ (red line) and actual proxy observations from La Selva (blue line). Series correlation coefficient r is 0.34 ($p < 0.05$, 63 effective degrees of freedom). (b) Climatological annual cycle for non-ENSO (closed circles) and ENSO (open circles) years from observations. (c) As in Figure 3b, except for model output.

mean levels, and the results are plotted versus the results using variable temperature and relative humidity. The scatter falls about a 1:1 line on the plot, indicating that the result is sensitive to neither temperature nor relative humidity variations. Grey lines, barely distinguishable from the results just described, show model output driven with mean precipitation but with relative humidity and temperature inputs whose variance is inflated by a factor of four. The corresponding plot, in which precipitation was held at mean 1985–2001 levels is shown in Figure 2c. In contrast with Figure 2b, the simulated variation is much reduced, suggesting that the result is quite sensitive to input precipitation variations.

[21] A comparison of simulated and observed $\delta^{18}O_{c,model}$ is in Figure 3a. Monthly-timescale correlation between simulated and observed time series is 0.34, significant for an estimated 63 effective degrees of freedom at the $p < 0.05$ significance level. Although the age model for the observed isotopic data was built from the most recent period back in time [*ES04*], agreement seems to be best in the earliest portion of the comparison time interval: correlation for the first 10 years is 0.45 ($p < 0.01$); and worst for the most recent 6 years ($r = 0.18$; $p = 0.78$). Figure 3b shows the average annual isotopic cycle in the isotopic observations [*ES04*, Figure 7c] for both normal and ENSO warm phase years (1986, 1991, 1997) within the comparison interval. As pointed out by *ES04* there is a statistically insignificant tendency toward lower isotopic values in July–August oxygen isotopic composition of cellulose during ENSO warm phase years. Figure 3c shows the same climatological isotopic values, for ENSO and non-ENSO years, but calculated from the model simulation shown in Figure 3a. The same but clearer result for ENSO warm phase versus normal years is found for the model: a two-sided t-test finds July–August average $\delta^{18}O_c$ values for ENSO and normal years significantly different ($t = 3.457$; $p < 0.01$), with most of the difference due to August values. I also note that simulated isotopic data for all years are enriched with respect to observations from January–April, and lighter with respect to observations from October–December (compare Figures 3b and 3c).

4. Discussion

4.1. Model Performance

[22] Despite a number of simplifying assumptions, parameterizations, fixed environmental and biological variables, and estimated quantities, the param-

eterized *BRFE04* model supports the *ES04* hypothesis for the environmental controls on the oxygen isotopic composition of tree-ring cellulose in tropical environments. Although large intramonthly variations in temperature and relative humidity are observed in the tropics [*Brenes*, 2003; *Lawrence et al.*, 2004], they are not readily evident on longer timescales in the boundary layer in the deep tropics [*Peixoto and Oort*, 1996]. In the absence of large variations in temperature and relative humidity at La Selva, the parameterized *BRFE04* system predicts cellulose isotopic variations dominated by a precipitation-induced amount effect, consistent with the hypothesis of *ES04* (Figures 2 and 3). Consequently, the simulated and observed annual cycles in the isotopic composition of wood cellulose at La Selva are similar (Figure 3), with annual variation in precipitation amount effect and evaporation [*ES04*] dominating the isotopic signal (Figure 2), especially for the earliest 10 years of record. Significant correlation of the time series is dominated by agreement of the annual cycle, which is partially guaranteed by the definition of the age model for the actual isotopic data [*ES04*] as a linear interpolation of isotopic measurements between minima observed in July climatological rainfall levels. However, the timing of isotopic maxima is not guaranteed by age model formulation, but was found to be similar and occurring during the dry season, roughly November–March (Figures 1 and 3). Further, the small and statistically nonsignificant ENSO warm phase isotopic anomaly (Figure 3c) was reproduced in the model simulations as a significantly lighter isotopic composition associated with higher average rainfall anomalies in July and August. These results suggest that the adaptation of *BRFE04* presented here is a fair description of the proxy system and its environmental controls, in particular the annual cycle of net precipitation and evaporation. On the basis of comparison of the simulated and observed isotopic data series, age model error in the particular observations studied here may be better than estimated by *ES04*, approaching ±1 year or less (Figure 3).

[23] There are also a number of important differences between model results and observations. First, correlation between time series (Figure 3) is higher in the earliest 10 years of the comparison interval (0.45; $p < 0.01$) than in the most recent 6 years (0.18; $p = 0.78$). This is surprising, as the age model for the observations was built from the most recent period backward in time, and integrated age model uncertainty is expected to increase back in time; but it clearly derives from the real and relatively weakly defined annual cycles of precipitation observed in the last few years of meteorological data (Figure 1). Unusual intermonthly variability in the La Selva precipitation data set for 1995–2001 is replicated in independent station data [*Bigelow and Ewel*, 2006] and in high resolution gridded precipitation data [*New et al.*, 2000]; a more regular annual cycle is observed in coarser-resolution gridded precipitation analyses [*Xie and Arkin*, 1997]. The reasons for these discrepancies are unknown. It is most likely that disagreement between simulations and observations is due to limitations of the isotopic observations, for example, the potential for missing years in the unreplicated record. If the model is indeed a fair description of the system, then replication (as used by *Treydte et al.* [2006]) ought to improve the fit between observations and simulations. Second, if biosynthetic fractionation ϵ_c is constant at 27‰, the +5.1‰ enrichment implied by fitting the two-component mixing model suggests that mean leaf or soil water evaporative enrichment may be underestimated in the simulations. Measurements of the isotopic composition of leaf and soil water and of precipitation are needed to constrain partitioning between mean leaf and soil water evaporative influences. Third, the observations are more highly autocorrelated than the simulations: lag-1 autocorrelations are 0.73 and 0.30, respectively. This suggests that in the real world, oxygen isotopic composition of cellulose is partially set on timescales longer than 1 month, possibly due to slow mixing of precipitation into soil moisture or storage of plant photosynthates. Both of these ideas are testable with soil water $\delta^{18}O$ measurements. Fourth, the model climatology systematically predicts higher $\delta^{18}O$ from January–March, and somewhat lower $\delta^{18}O$ values in September–December. The early and late period differences may be due to an unobserved growth hiatus during this period, which corresponds to the dry season at La Selva. Band dendrometer measurements might be used to resolve this possibility. Alternatively, it might be due to biochemical effects at the intramolecular level which have recently been hypothesized to limit evaporative enrichment effects when source water $\delta^{18}O$ is heavier than about −10‰ [*Sternberg et al.*, 2006]. Parameterized source water $\delta^{18}O$ estimates (section 2.2) exceed this value during the early and late months of the year.

4.2. Model Sensitivity

[24] Simulations of annual and interannual variations in cellulose isotopic composition are relatively

insensitive to parameter values (Tables 1 and 2 and Figure 2a) as estimated by the 1000-member Monte Carlo sampling of the 17-dimensional parameter space. The signal to parameter noise ratio is about 8.7 (Figure 2a; section 3). The importance of source water isotopic variations is again evident from a comparison of simulated δ and Δ values for water vapor, evaporation site water, leaf water (which includes evaporation site and Peclet effects), and cellulose components (results not shown). The Δ values, which do not include simulated source water isotopic variations (section 1), are an order of magnitude smaller than the δ values, and cannot explain the variation observed in the actual isotopic data from La Selva. Experiments magnifying the observed amplitude of relative humidity and temperature variations by a factor of 4 while holding precipitation fixed also indicate that the simulated isotopic variations are not sensitive to uncertainties in observations and estimation of relative humidity and temperature (section 2 and Figures 1 and 2b). Additional experiments, in which stomatal conductance, transpiration rate, boundary layer diffusive fractionation, total diffusive fractionation, and leaf temperature were varied for artificially large amplitudes were together able to explain only about 20% of the observed variance (results not shown). Overall, sensitivity experiments suggest that the analysis of variance in the simulations is not sensitive to model formulation, choice of fixed parameters, and observed temperature and estimated relative humidity variations. The only parameters to which the modeled mean and variance were sensitive were the amount effect and leaf temperature parameters c_{1-4} (results not shown). Hence, if strong inferences are to be made concerning the mean value of the isotopic record, these parameterizations should be more tightly constrained with direct observations.

4.3. Applications

[25] A more general modeling experiment illustrates the potential of forward modeling for objective identification and extraction of unbiased, climatically forced features in proxy paleoclimatic observations. For the specific case of stable isotopes in tropical trees, prediction of the amplitude of the annual cycle and interannual variation in precipitation represents a testable hypothesis for interpretation of proxy observations, and can inform paleoclimatic sampling network design and replication strategies for reconstruction of large-scale phenomena such as ENSO. In Figure 4 the *BRFE04* model has been run using as input gridded precipitation, temperature, and vapor pressure [*New et al.*, 2000; *Bolton*, 1980] for the past century. At each grid point, the annual cycle has been removed from the results to form climatological anomalies, and the anomalies annually averaged, prior to correlation analysis. Figure 4a shows in colors the correlation of the first principal component of annually averaged tropical (30°N–30°S) sea surface temperature anomalies with model δ^{18}O; contours show the correlation of the first principal component of the δ^{18}O model with tropical SST anomaly. Here the leading pattern in the isotope model output is associated with ENSO, and the leading pattern in tropical SST is associated with isotope model variability across broad regions of the terrestrial tropics. Figure 4b shows the same results except that the isotope model output has been replaced by gridded precipitation data; the patterns are similar to those in Figure 4a. Figure 4c gives results for the period 1951–2002, and Figure 4d gives results in which the EOF patterns derived in Figure 4c have been projected on the data for 1901–1950; in both of these cases, correlations not significant at the 95% level have been masked out. *Vuille and Werner* [2005] and *Hoffman et al.* [1998] showed broadly similar results based on

Figure 4. Simulations of isotopes in trees for the global tropics, 30N–30S, 1901–2002, April–March annually averaged anomalies, based on gridded precipitation, temperature, and vapor pressure [*New et al.*, 2000], using relative humidity calculated from vapor pressure and temperature following *Bolton* [1980], and isotope model parameters listed in Tables 1 and 2. (a) Correlation (colors) of simulated isotope records with first principal component of tropical (30N-30S) SST [*Kaplan et al.*, 1998]; correlation (contours) of first principal component of simulated isotope records with gridded SST. Correlations of >|0.3| are significant at the $p < 0.05$ level assuming 45 effective degrees of freedom. (b) As in Figure 4a, except replacing modeled isotope records with −1*precipitation from *New et al.* [2000]. Simulations are dominated by precipitation amount; their leading pattern of variation is associated with ENSO. (c) As in Figure 4a, except for EOF analyses performed over the 1951–2002 period, and showing only significant correlations ($r > |0.4|$; $p < 0.05$) (“Calibration”). (d) As in Figure 4c, except with SST and isotope model correlations calculated for the 1901–1950 period on the basis of principal components calculated by projection of the calibration period 1st EOF patterns on the 1901–1950 data (“Verification”). Figures 4c and 4d suggest that precipitation variability associated with ENSO may be retrieved from a sampling of a limited set of regions within the global tropics, and represent a hypothesis testable with observations. (e) Color scale used to plot Figures 4a–4d.

the IAEA database of isotopes in precipitation (http://isohis.iaea.org) and atmospheric circulation modeling experiments over shorter timescales.

[26] Comparison of Figures 4c and 4d suggests that if the isotope model is a fair description of reality, then a network of tropical tree isotope series from tropical South America, and Australasia may resolve variability in precipitation associated with ENSO. Of course, this result assumes, for instance, that the amount effect in precipitation is similar across the global tropics, and this is not true. However, the model can be run with parameters adjusted to represent specific locales for which paleoenvironmental reconstructions based on oxygen isotopes in tree-rings are being considered. Modeling exercises can suggest to what extent, for example, temperature, humidity and precipitation influences compete to determine the observed stable isotope records. Alternatively, if we assume

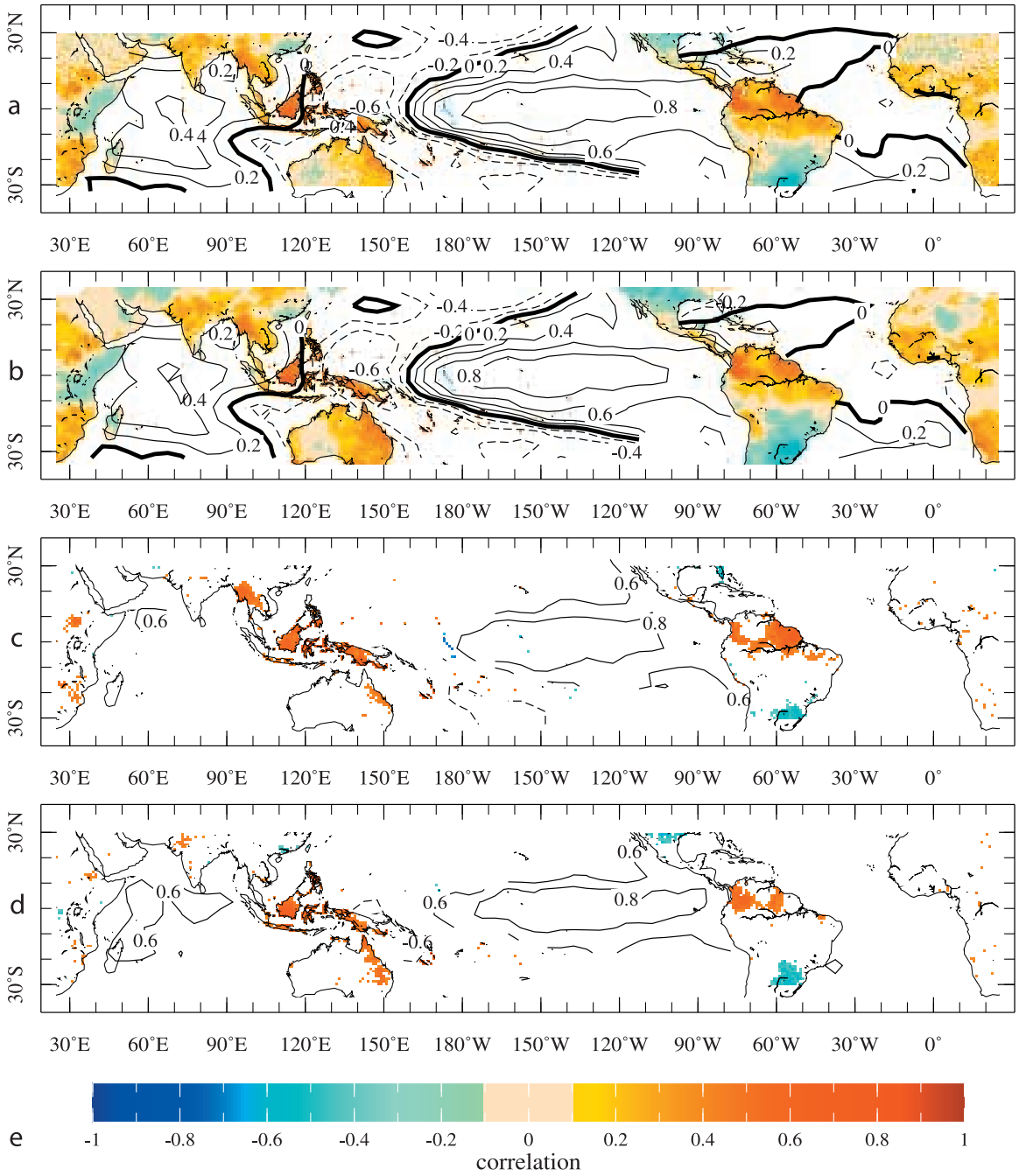

Figure 4

the simulations are a good description of the proxy system, they may be used to test calibration period age modeling [*Anderson et al.*, 2002; *Treydte et al.*, 2006]. As an example of the latter approach, a composite from two Samanea Saman $\delta^{18}O$ data series [*Poussart et al.*, 2004, Figure 5a] is significantly ($p < 0.05$) correlated with $\delta^{18}O$ simulations (Figure 4) from East Java and Borneo and with NINO34 SST anomaly, if the earliest 8 years of the composite age model are linearly stretched to 10 years (results not shown). More generally, spatial, temporal and spectral forward model–proxy data intercomparisons can be used as an important complement to inverse modeling for ground-truthing the strengths and limitations of proxy-based paleoclimatic reconstructions [*Schmidt*, 1999]. For example, the simplified empirical calculation of water vapor and precipitation $\delta^{18}O$ could be replaced by the output of general circulation models of the atmosphere fitted with stable isotope modules [*Joussame et al.*, 1994]; the coupled climate-proxy model could then be used to compare climate model integrations to proxy precipitation series.

5. Conclusions

[27] A mechanistic model of the oxygen isotopic composition of tree cellulose, parameterized as a time series function of monthly precipitation, air temperature, and relative humidity, is employed to simulate the primary features observed in actual oxygen isotopic data from a wet tropical environment. The simulations are crudely consistent with a system in which the isotopic composition of cellulose is determined predominantly by tropical precipitation amount. A modeling exercise for the global tropics supports the eventual recovery of interannual rainfall variability associated with ENSO from replicated stable isotope measurements from trees located in selected tropical environments worldwide, and represents a hypothesis testable with actual isotopic data. The time series extension of the isotope model is freely available. It is hoped that this tool will permit more quantitative integration of forward models into paleoclimatological data interpretation, and potentially to identify opportunities for continued modeling studies.

Acknowledgments

[28] This work was inspired by an invitation from Emi Ito and Yongsong Huang to present at the American Geophysical Union Fall 2005 Meeting and was supported by NSF grant ATM-0349356. I thank OTS/OET for making the meteorological data available via anonymous ftp and M. M. Barbour, J. S. Roden, G. D. Farquhar, and J. R. Ehleringer for making their model available via the Internet. T. E. Huxman helped sort the details of the dynamic stomatal conductance module of the model. S. W. Bigelow and J. J. Ewel kindly provided unpublished stomatal conductance and vapor pressure deficit data sets and advised on their reduction and interpretation. M. B. Blumenthal provided the data and computational platform used to develop and plot Figure 4 via Ingrid and the IRI Climate Data Library (http://iridl.ldeo.columbia.edu). M. H. Gagen, K. J. Anchukaitis, P. F. Poussart, L. D. Labeyrie, T. E. Huxman, G. D. Farquhar, and two anonymous reviewers provided helpful comments on manuscript drafts.

References

Anderson, W. T., S. M. Bernasconi, J. A. McKenzie, M. Saurer, and F. Schweingruber (2002), Model evaluation for reconstructing the oxygen isotopic composition in precipitation from tree ring cellulose over the last century, *Chem. Geol.*, *182*, 121–137.

Aphalo, P. J., and P. G. Jarvis (1991), Do stomata respond to relative humidity?, *Plant Cell Environ.*, *14*, 127–132.

Barbour, M. M., J. S. Roden, G. D. Farquhar, and J. R. Ehleringer (2004), Expressing leaf water and cellulose oxygen isotope ratios as enrichment above source water reveals evidence of a Péclet effect, *Oecologia*, *138*, 426–435, doi:10.1007/s00442-003-1449-3.

Bigelow, S. W. (2001), Evapotranspiration modeled from stands of three broad-leaved tropical trees in Costa Rica, *Hydrol. Processes*, *15*, 2779–2796.

Bigelow, S. W., and J. J. Ewel (2006), Vapor pressure deficit, stomatal conductance for *Hieronyma alchorneoides*, rainfall, relative humidity, temperature for 1993–2001, report, U.S. Natl. Sci. Found., Washington, D. C.

Bolton, D. (1980), The computation of equivalent potential temperature, *Mon. Weather Rev.*, *108*, 1046–1053.

Bowen, G., and B. Wilkinson (2002), Spatial distribution of $\delta^{18}O$ in meteoric precipitation, *Geology*, *30*, 315–318.

Brenes, T. (2003), Meteorological Data at La Selva Biological Station. Long Term Records since 1957, http://www.ots.ac.cr/en/laselva/metereological.shtml, Organ. for Trop. Stud., Durham, N. C.

Butterfield, R., and M. Espinosa (2003), Parcelas de Canada: Adaptabilidad de 13 Especies Nativas Maderables Bajo Condiciones de Plantacion en las Tierras Bajas Humedas del Atlantico, Costa Rica, http://www.ots.ac.cr/es/projects/trials/cana_sp.htm, Organ. for Trop. Stud., Durham, N. C.

Evans, M. N., and D. P. Schrag (2004), A stable isotope-based approach to tropical dendroclimatology, *Geochim. Cosmochim. Acta*, *68*, 3295–3305.

Fairbanks, R. G., M. N. Evans, J. L. Rubenstone, R. A. Mortlock, K. Broad, M. D. Moore, and C. D. Charles (1997), Evaluating climate indices and their geochemical proxies measured in corals, *Coral Reefs*, *16*, S93–S100.

Gonfiantini, R., M.-A. Roche, J.-C. Olivy, J.-C. Fontes, and G. M. Zuppi (2001), The altitude effect on the isotopic composition of tropical rains, *Chem. Geol.*, *181*, 147–167.

Hoffman, G., M. Werner, and M. Heimann (1998), Water isotope modeule of the ECHAM atmospheric general circulation model: A study on timescales from days to several years, *J. Geophys. Res.*, *103*, 16,871–16,896.

Jarvis, P. G., and K. G. McNaughton (1986), Stomatal control of transpiration: Scaling up from leaf to region, *Adv. Ecol. Rese.*, *15*, 1–19.

Joussame, S., R. Sadourny, and J. Jouzel (1994), A general circulation model of water isotope cycles in the atmosphere, *Nature*, *311*, 24–29.

Kaplan, A., M. A. Cane, Y. Kushnir, A. C. Clement, M. B. Blumenthal, and B. Rajagopalan (1998), Analyses of global sea surface temperature 1856–1991, *J. Geophys. Res.*, *103*, 18,567–18,589.

Lachniet, M. S., and W. P. Patterson (2006), Use of correlation and stepwise regression to evaluate physical controls on the stable isotope values of Panamanian rain and surface waters, *J. Hydrol.*, *324*, 115–140.

Lawrence, J. R., S. D. Gedzelman, D. Dexheimer, H.-K. Cho, G. D. Carrie, R. Gasparini, C. R. Anderson, K. P. Bowman, and M. I. Biggerstaff (2004), Stable isotopic composition of water vapor in the tropics, *J. Geophys. Res.*, *109*, D06115, doi:10.1029/2003JD004046.

Linacre, E. T. (1964), A note on a feature of leaf and air temperatures, *Agric. Meteorol.*, *1*, 66–72.

Lohammar, T., S. Larsson, S. Linder, and S. O. Falk (1980), FAST-simulation models of gaseous exchange in Scots pine, *Ecol. Bull.*, *32*, 505–523.

Majoube, M. (1971), Fractionnement en oxygéne et en deutèrium ente l'eau et sa vapeur, *J. Chim. Phys. Phys. Chim. Biol.*, *68*, 1423–1436.

New, M., M. Hulme, and P. Jones (2000), Representing twentieth-century space-time climate variability. Part II: Development of 1901–96 monthly grids of terrestrial surface climate, *J. Clim.*, *12*, 2217–2238.

Peixoto, J. A., and A. H. Oort (1996), The climatology of relative humidity in the atmosphere, *J. Clim.*, *9*, 3443–3463.

Poussart, P. F., M. N. Evans, and D. P. Schrag (2004), Resolving seasonality in tropical trees: Multi-decade, high-resolution oxygen and carbon isotope records from Indonesia and Thailand, *Earth Planet. Sci. Lett.*, *218*, 301–316.

Reich, A., N. Holbrook, and J. J. Ewel (2004), Developmental and physiological correlates of leaf size in *Hyeronima alchorneoides* (Euphorbiaceae), *Am. J. Bot.*, *91*, 582–589.

Roden, J. S., G. Lin, and J. R. Ehleringer (2000), A mechanistic model for interpretation of hydrogen and oxygen ratios in tree-ring cellulose, *Geochim. Cosmochim. Acta*, *64*, 21–35.

Saurer, M., K. Aellen, and R. Siegwolf (1997), Correlating $\delta^{13}C$ and $\delta^{18}O$ in cellulose of trees, *Plant Cell Environ.*, *20*, 1543–1550.

Schmidt, G. A. (1999), Forward modeling of carbonate proxy data from planktonic foraminifera using oxygen isotope tracers in a global ocean model, *Paleoceanography*, *14*, 482–497.

Sternberg, L. D. L., M. C. Pinzon, W. T. Anderson, and A. H. Jahren (2006), Variation on oxygen isotope fractionation during cellulose synthesis: Intramolecular and biosynthetic effects, *Plant Cell Environ.*, *29*, 1881–1889, doi:10.1111/j.1365-3040.2006.01564.

Subcommittee on Global Change Research (2003), Strategic plan for the Climate Change Science Program, final report, U.S. Clim. Change Sci. Program, Washington, D. C. (Available at http://www.climatescience.gov/Library/stratplan2003/final/default.htm.)

Treydte, K. S., G. H. Schleser, G. Helle, D. C. Frank, M. Winiger, G. H. Haug, and J. Esper (2006), The twentieth century was the wettest period in northern Pakistan over the past millennium, *Nature*, *440*, 1179–1182.

Verheyden, A., G. Helle, G. H. Schleser, F. Dehairs, H. Beeckman, and N. Koedam (2004), Annual cyclicity in high-resolution stable carbon and oxygen isotope ratios in the wood of the mangrove tree Rhizophora mucronata, *Plant Cell Environ.*, *27*, 1525–1536.

Vuille, M., and M. Werner (2005), Stable isotopes in precipitation recording South American summer monsoon and ENSO variability: Observations and model results, *Clim. Dyn.*, *25*, 401–413.

Wallace, J. M., and P. V. Hobbs (1997), *Atmospheric Science: An Introductory Survey*, Elsevier, New York.

Waterhouse, J. S., V. R. Switsur, A. C. Barker, A. H. C. Carter, and I. Robertson (2002), Oxygen and hydrogen isotope ratios in tree rings: How well do models predict observed values?, *Earth Planet. Sci. Lett.*, *201*, 421–430.

Xie, P.-P., and P. A. Arkin (1997), Global precipitation: A 17-year monthly analysis based on gauge observations, satellite estimates, and numerical model outputs, *Bull. Am. Meteorol. Soc.*, *78*, 2539–2558.